Am J Cancer Res 2023;13(5):2013-2029
www.ajcr.us /ISSN:2156-6976/ajcr0148232

Original Article

Selective activation of TGFβ signaling by *P. gingivalis*-mediated upregulation of GARP aggravates esophageal squamous cell carcinoma

Shegan Gao[1,2*], Ke Liu[2*], Yelin Jiao[1], Pan Chen[1], Bianli Gu[1], Yiwen Liu[1], Gaofeng Liang[1], Linlin Shi[1], Fuyou Zhou[3], Richard J Lamont[4], Huizhi Wang[5], Yi-Jun Qi[1]

[1]State Key Laboratory of Esophageal Cancer Prevention & Treatment, Henan Key Laboratory of Microbiome and Esophageal Cancer Prevention and Treatment, Henan Key Laboratory of Cancer Epigenetics, Cancer Hospital, The First Affiliated Hospital, College of Clinical Medicine, Medical College of Henan University of Science and Technology, Luoyang 471003, Henan, China; [2]School of Information Engineering, Henan University of Science and Technology, Luoyang 471003, Henan, China; [3]Department of Thoracic Surgery, Anyang Tumor Hospital, Anyang 455000, Henan, China; [4]Department of Oral Immunology and Infectious Diseases, University of Louisville School of Dentistry, Louisville, KY 40202, USA; [5]VCU Philips Institute for Oral Health Research, Department of Oral and Craniofacial Molecular Biology, Virginia Commonwealth University, Richmond, VA 23298, USA. [*]Equal contributors.

Received December 4, 2022; Accepted April 21, 2023; Epub May 15, 2023; Published May 30, 2023

Abstract: Aberrant TGFβ signaling plays critical roles in the progression of multiple cancers; however, the functional mechanism of this signaling network in the infectious milieu of Esophageal Squamous Cell Carcinoma (ESCC) remains largely unknown. In this study, by using global transcriptomic analysis, we found that *Porphyromonas gingivalis* infection increased TGFβ secretion and promoted the activation of TGFβ/Smad signaling in cultured cells and in clinical ESCC samples. Furthermore, we demonstrated for the first time that *P. gingivalis* enhanced the expression of Glycoprotein A repetitions predominant (GARP), thereby activating TGFβ/Smad signaling. Moreover, the increased GARP expression and the subsequent TGFβ activation was partially dependent on the fimbriae (FimA) of *P. gingivalis*. Intriguingly, eliminating *P. gingivalis*, inhibiting TGFβ, or silencing GARP led to a decreased phosphorylation of Smad2/3, the central mediator of TGFβ signaling, as well as an attenuated malignant phenotype of ESCC cells, indicating that the activation of TGFβ signaling could be an adverse prognostic factor of ESCC. Consistently, our clinical data demonstrated that the phosphorylation of Smad2/3 and the expression of GARP were positively correlated to the poor prognosis of ESCC patients. Lastly, using xenograft models, we found that *P. gingivalis* infection remarkably activated TGFβ signaling and subsequently enhanced the tumor growth and lung metastasis. Collectively, our study indicated that TGFβ/Smad signaling mediates the oncogenic function of *P. gingivalis* in ESCC, which is augmented by the expression of GARP. Therefore, targeting either *P. gingivalis* or GARP-TGFβ signaling could be a potential treatment strategy for patients with ESCC.

Keywords: TGFβ, *Porphyromonas gingivalis*, esophageal cancer, GARP

Introduction

Studies have shown that genetically modified mice that are susceptible to cancer develop significantly fewer tumors under germ-free conditions than under regular condition [1, 2]. Consistently, the administration of metronidazole, an anaerobic antibiotic, leads to an apparent amelioration of various cancers in multiple tumor models [3-5]. These studies strongly suggest the existence of pro-tumorigenic bacteria in local bacterial microbiome. Intriguingly, recent findings have demonstrated the colonization of some bacteria, such as *Streptococcus gordonii* and *Holdemanella biformis*, suppress the pro-tumorigenic phenotypes in epithelial cells [6-8]. In addition, recent studies have also shown that eliminating *Gammaproteobacteria* or *Fusobacterium nucleatum* is able to reverse chemoresistance and substantially improve the prognosis of patients with colorectal cancer [4, 5, 9], indicating the pro-carcinogenic properties

of these bacteria. *Porphyromonas gingivalis* is a gram-negative bacterium found in the human oral cavity and is considered a keystone bacterium for oral microbiome dysbiosis. In addition, our and other previous studies have discovered that *P. gingivalis* also colonizes the esophagus mucosa and is associated with multiple gastrointestinal cancers [3, 10, 11]. Furthermore, our recent study has demonstrated that *P. gingivalis* is enriched in the esophageal cancer tissue compared to normal tissue, contributing to the increased cancer metastasis and the resistance to chemotherapy, thereby leading to the poor prognosis of patients with esophageal squamous cell carcinoma (ESCC) [3, 12]. Moreover, other studies have indicated that *P. gingivalis* can promote epithelial mesenchymal transition (EMT) as well as the expression of stem cell markers [6, 13] and can downregulate the anti-tumor immune responses [14, 15]. Although growing evidence demonstrates the pro-tumorigenic properties of *P. gingivalis* in orodigestive cancers, the molecular mechanisms underlying the function of *P. gingivalis* in ESCC remains largely unknown. Therefore, identifying key molecular targets modified by *P. gingivalis* in ESCC will shed light on the therapeutic application of targeting *P. gingivalis* for the control of this malignant disease.

Transforming growth factor beta (TGFβ), a ubiquitously expressed cytokine, plays a key role in cell proliferation, differentiation, angiogenesis, immune responses, and carcinogenesis. The activation of TGFβ signaling is initiated by the hierarchical binding of TGFβ to its receptor, TGFβ type I receptor (TbR-1) and type II receptor (TbR-II) [16, 17], which recruits and phosphorylates the downstream receptor-activated Smads (R-Smads), Smad2 and Smad3, at their C-terminal SSXS domain [18, 19]. Phosphorylated Smad2/3 (pSmad2/3) can then form a complex with co-Smad (Smad4) and translocate to the nucleus where the Smad complex regulates the transcription of target genes in cooperation with other nuclear cofactors [20]; therefore, pSmad2/3 is frequently used as the indicator of the activated TGFβ signal cascade. Notably, through interacting with different signaling pathways involved in EMT or cancer cell stemness, the activated TGFβ signaling can play a tumor suppressing or a tumor promoting role, depending on the type and stage of the cancer [21-23]. Cancer cells therefore frequently escape TGFβ-mediated growth inhibition but take the advantage of other TGFβ-mediated growth promoting activities. Nevertheless, TGFβ is frequently overexpressed in solid tumor tissues, and aberrant TGFβ signaling is associated with the progression of multiple gastrointestinal cancers [24-29]. Although the abundance of TGFβ and Smad2/3 phosphorylation have been used as prognostic markers for various cancers, the possible influence of infectious agents on the activation of TGFβ signaling in ESCC, as well as the underlying mechanisms involved remain largely unknown.

In mammalian cells, TGFβ exists in different forms such as soluble active TGFβ, LTGFβ, and cell surface TGFβ [30, 31]. Glycoprotein A repetitions predominant (GARP) is a transmembrane protein widely expressed on human cancer cells that acts as a docking receptor for latent TGFβ (LTGFβ) to promote TGFβ activation. GARP is recently found to be upregulated in a variety of cancers and promotes cancer invasion, EMT, immune tolerance, as well as metastasis via activating LTGFβ [32]. Other studies have also reported that GARP is expressed on $Foxp3^+$ regulatory T cells (Treg) and robustly enhances their suppressive function, leading to cancer evasion from immune surveillance. While the increased expression of GARP and its pro-tumorigenic function have been reported in several cancers including breast, lung, melanoma, bone sarcoma, and colon cancers [33-36], its expression and its possible role in the progression of ESCC remain to be determined. In addition, the function and regulation of GARP in ESCC are also unknown.

In this study, we demonstrated for the first time that *P. gingivalis* infection promoted the activation of TGFβ signaling and enhanced the malignant phenotype of ESCC in both cultured ESCC cells and mouse tumor models. In addition, we found that *P. gingivalis* augmented TGFβ activation through upregulating GARP expression in a fimbriae-dependent manner. Moreover, we found that Smad2/3 phosphorylation and the upregulation of GARP were positively associated with a poor prognosis of ESCC patients. Taken together, these results not only demonstrated the TGFβ signaling-mediated pro-tumorigenic property of *P. gingivalis,* but also revealed the role of GARP in this process.

Materials and methods

Clinical specimens

In total, 190 ESCC samples were collected from the First Affiliated Hospital of Henan University of Science & Technology and Anyang People's Hospital between 2012 and 2017. All ESCC cases were confirmed by histopathology and underwent curative esophagectomy without preoperative neoadjuvant chemoradiotherapy. The clinical data of the 190 patients were presented in Table S2. This study was approved by the Ethics Committee of the First Affiliated Hospital of Henan University of Science & Technology. Written informed consent was obtained from all patients.

Bacterium and cell culture

Human ESCC cell lines NE6-T and KYSE30 were cultured in Roswell Park Memorial Institute (RPMI) 1640 medium supplemented with 10% fetal bovine serum (FBS), 100 units/mL penicillin G, and 100 μg/mL streptomycin in a 37°C humidified incubator with 5% CO_2. *P. gingivalis* strain ATCC 33277 and its derivative *fimA*-mutant were cultured in trypticase soy broth supplemented with yeast extract (1 mg/mL), hemin (5 μg/mL), and menadione (1 μg/mL), at 37°C under anaerobic conditions with 85% N_2, 10% H_2, and 5% CO_2.

Western blot analysis

Cells were lysed in RIPA lysis buffer, and protein concentrations were quantified by a BCA protein assay kit. Protein samples were resolved by SDS-PAGE and then transferred onto PVDF membranes. The membranes were blocked with 5% fat-free dry milk for 1 h and then incubated with indicated primary antibodies at 4°C overnight. Primary antibodies against the following proteins were used in this study: Smad2/3 (1:500, CST, 8658), pSmad2/3 (1:200, CST, 8828), GARP (1:100, GeneTex, GTX81794), TLR4 (1:500, Abcam, 13556), MYD88 (1:250, Abcam, 28763), Oct4 (1:400, Proteintech, 11263-1-AP, Proteintech), Snail (1:200, CST, 3879), E-cadherin (1:200, CST, 14472), N-cadherin (1:500, CST, 14215), PAI-1 (1:800, CST, 11907), and GAPDH (1:1000, EARTH, E021010-01). After incubation with HRP-conjugated secondary antibodies for 1 h at room temperature, the signals were visualized using Supersignal West chemiluminescent substrate (Pierce Biotechnology, Rockford, IL, USA) and quantified using image analysis software.

Immunofluorescence (IF) staining

NE6-T and KYSE30 cells were seeded on confocal glass bottom dishes and treated as indicated. The cells were then fixed in 4% paraformaldehyde for 30 minutes at room temperature, permeabilized with 0.5% Triton-X100 for 10 minutes, and blocked with 5% BSA, followed by incubation with primary antibodies. The staining signal was developed using fluorophore-conjugated secondary antibodies and examined under a Zeiss LSM700 confocal microscope. DAPI was used for nuclear counterstaining. The primary antibodies used in this study were anti-Oct4 (1:200, CST, 2840), -Smad2/3 (1:200, CST, 8658) and -GARP (1:250, GeneTex, GTX81794).

ELISA assay

Conditioned media and xenograft tumor samples were collected for total and active TGF-β1 measurement using LEGEND MAX Free Active TGF-β1 ELISA Kit with Pre-coated Plates (Biolegend, San Diego, CA, USA) or human total TGF-β1 ELISA Kit (ExCell Bio, Shanghai, China) according to the manufacturer's protocols.

Quantitative real-time PCR

Total RNA was extracted from cells using Trizol reagent (Invitrogen) and was reverse transcribed into cDNA using a Reverse Transcription System (Promega) following the manufacturer's instructions. Quantitative real-time PCR was performed in triplicate on an Applied Biosystems 7900 quantitative PCR system (Foster City, CA, USA). Relative mRNA expression was normalized to GAPDH expression. The sequences of primers used in this study were listed in Table S3.

Immunohistochemistry (IHC) staining

Formalin-fixed, paraffin-embedded (FFPE) tumor tissue blocks were sliced into 5 μm sections. The tissue sections were rehydrated, and the antigen was retrieved using citrate buffer treatment (10 nmol/L [pH 6]) at 100°C for 15 min. Endogenous peroxidase was blocked

using 3% hydrogen peroxide. IHC staining was performed using the streptavidin-biotin-peroxidase complex method. The immunostaining scores were obtained by multiplying the staining intensity and the percentage of positive cells.

Luciferase reporter assay

NE6-T and KYSE30 cells were transfected with SMAD Cignal reporter (QIAGEN) by Lipofectamine 2000 reagent (Invitrogen). The activities of firefly luciferase and renilla luciferase were measured 48 h after transfection using the Dual-Luciferase Reporter Assay System (Promega, WI) according to the manufacturer's protocol. The relative promoter activity was presented as the ratio of firefly luminescence value to renilla luminescence value.

High-throughput sequencing

Total RNA was isolated from KYSE30 cells that were co-cultured with either *P. gingivalis* or PBS (negative control) and were used for library preparation. Sequencing was performed on an Illumina Hiseq 4000 (San Diego, CA, USA) for 2 × 150 bp paired-end configuration. The sequencing data was analyzed using TopHat-HTSeq-DeSeq2frame. Raw reads were processed through quality control and genome mapping used the DESeq2 package (v1.30.1). Differentially expressed genes were determined using a cutoff false discovery rate (FDR) < 0.05. The RNA sequencing data have been deposited in NCBI's GEO with accession number GSE 121995. For subnetwork construction, 245 differentially expressed genes were mapped and imported to NetBox (http://cbio.mskcc.org/tools/index.html) that queried the human protein-protein interaction network for interaction between linkers and seeds.

Cell proliferation assay

Cell viability was measured by MTT assay. Briefly, cells (2,000 cells/well) were seeded in triplicate into 96-well plates and co-cultured with wild-type *P. gingivalis*, *fimA*-mutant, or PBS at a multiplicity of infection of 1:10. At indicated time points, MTT solution was added to each well and incubated for 4 h. The optical density (OD) value at 490 nm was determined using a microplate spectrophotometer (PerkinElmer, Waltham, MA, USA).

Mouse xenograft tumor model

Male BALB/c athymic nude mice (4 weeks old) were purchased from Charles River Bioscience Co. Inc, China. NE-6 T and KYSE30 cells were incubated with wild-type *P. gingivalis*, *fimA*-mutant, or PBS at a multiplicity of infection of 1:10 for 24 h and then harvested for xenograft tumor formation. Specifically, cells of 3×10^6/100 ul PBS were injected subcutaneously into the flanks or intravenously into the tail veins of mice (n=6 per group). Tumor growth was monitored daily, and the tumor dimensions were measured every 3 days using a digital caliper. Bioluminescence imaging of tail vein injected mice was performed weekly to evaluate tumor metastasis. Tumor volume was calculated as volume (mm^3) = $L \times W^2/2$. To study the effect of a TGFβ receptor kinase inhibitor (SB-431542) or antibiotics (tinidazole) on tumor growth, mice that were inoculated with *P. gingivalis*-infected cells by subcutaneous or tail vein injection were randomly divided into two groups (n=6 mice/per group) and were treated with either SB-431542 (0.5 mg/kg) or tinidazole (15 mg/kg) by intraperitoneal injection twice a week for six weeks. At the end of the experiment, the mice were anesthetized and euthanized, and all tumors were harvested for H&E, IHC, ELISA, and PCR analyses. All animal studies were approved by the Institutional Animal Care and Use Committee of the First Affiliated Hospital of Henan University of Science & Technology, and all mouse experiments were performed in accordance with the National Institute of Health Guidelines for the Care and Use of Laboratory Animals.

Statistical analysis

Statistical analyses were conducted using GraphPad (GraphPad software 9) or R. Unpaired/paired Student's t test or Man-Whitney U test (two tailed) were used to compare statistical significance between two groups where appropriate. One way ANOVA tests with Dunnett's method was performed for comparing more than two groups, and two-way ANOVA test was utilized to analyze the tumor growth with multiple variables. The associations among categorical variables of patients were analyzed using chi-square test or Fisher's exact test. The Kaplan-Meier curves and log-rank tests were used to assess the statistical significance of

overall survival. All data were presented as the mean ± SD of three independent experiments. *P* values less than 0.05 were considered statistically significant and were noted as $*P < 0.05$, $**P < 0.01$, $***P < 0.001$.

Results

Transcriptome analysis of esophageal cancer cells upon challenging with P. gingivalis

It is known that infection with *P. gingivalis* leads to a wide range alteration of host cell machinery which is associated with a variety of pathogenic responses. Our previous studies have demonstrated that *P. gingivalis* colonization aggravates ESCC through modulating cell cycle machinery and promoting cancer cell chemotherapy resistance [3, 12]. To comprehensively understand the molecular changes induced by *P. gingivalis* infection in esophageal cancer cells, we utilized *P. gingivalis*-stimulated KYSE30 cells, a representative ESCC cell line, to examine the alteration of transcriptomic profile upon *P. gingivalis* challenge. We identified 245 differentially expressed genes (fold change > 1.5) upon *P. gingivalis* challenge from 3 independent experiments (**Figure 1A**; Table S1). Further Kyoto Encyclopedia of Genes and Genomes (*KEGG*) analysis indicated these genes were enriched in TGFβ signaling, Hippo signaling, and phosphatidylinositol 3-kinase (PI3K)/Akt signaling pathway (**Figure 1B**).

P. gingivalis infection upregulated TGFβ activity and the phosphorylation of Smads

Aberrant TGFβ signaling has been shown in a variety of cancers with either tumor-inhibiting or tumor-promoting effect, depending on tumor stages, e.g., early or late stage [37]. Given that TGFβ activation was observed in ESCC cells in our transcriptomic profiling, we next examined the impact of *P. gingivalis* infection on the secretion of TGFβ ligand and the activation of TGFβ/Smad signaling. As shown in **Figure 1C**, the total and active TGFβ1 levels in the conditioned media of *P. gingivalis*-treated KYSE30 and NE6-T cells were significantly elevated compared with that in the media of untreated control cells. Additionally, *P. gingivalis* increased the activity of a TGFβ-responsive Smad-binding element (SBE) luciferase reporter in KYSE30 and NE6-T cells at 24 h post infection (**Figure 1D**). To further confirm that the increased SBE activity was caused by the elevated TGFβ level from *P. gingivalis* infection, we utilized TGFβ1 neutralizing antibody (TGFβ1-N), TGFβ receptor kinase inhibitor SB-431542, or tinidazole, an anaerobic bacterial antibiotic, to suppress TGFβ signaling or eliminate *P. gingivalis* stimuli. As expected, the increased luciferase activity was abolished by pretreatments with each of these inhibitors (**Figure 1D**). Consistently, real-time PCR verified the transcriptional induction of TGFβ target genes, including plasminogen activator inhibitor-1 (PAI-1) and Smad7, were attenuated by TGFβ1-N, SB-431542, or tinidazole in *P. gingivalis*-treated KYSE30 and NE6-T cells (**Figure 1E**). In line with these, *P. gingivalis*-induced TGFβ/Smad2/3 activity was confirmed by the enhanced phosphorylation (**Figure 1F**) and nuclear accumulation (**Figure 1G**) of Smad2/3 and Oct4, which could also be abolished by TGFβ1-N, SB-431542, and tinidazole. Altogether, our results demonstrated that *P. gingivalis* infection significantly enhanced the secretion of TGFβ and subsequently activated TGFβ/Smads signaling in ESCC cells.

P. gingivalis-mediated upregulation of GARP enhanced TGFβ activation through TLR4/MyD88 signaling

Next, we explored how *P. gingivalis* activates TGFβ signaling in ESCC cells. It has been well known that the latent TGFβ goes through several steps to release active TGFβ [30] which then binds to TbR1 and TbR2 to activate the downstream Smad proteins [30]. On the other hand, recent studies have revealed that the expression of GARP on Treg cells can enrich active TGFβ on cell surface and the subsequent activation of Smads signaling cascade [32]. Since our transcriptomic data and *in vitro* experimental data indicated that *P. gingivalis* infection upregulated TGFβ level, we questioned the effect of *P. gingivalis* infection on GARP expression in ESCC cells. We found that GARP protein levels were robustly increased in *P. gingivalis*-infected KYSE30 and NE6-T cells (**Figure 2A**). To further determine whether GARP is required for the activation of TGFβ signaling, we knocked down GARP by specific siRNA and found that GARP silencing abrogated the *P. gingivalis*-induced increase of active TGFβ in KYSE30 and NE6-T cells (**Figure 2B**). Consistent with this, SBE luciferase reporter activity was also reduced by GARP knockdown (**Figure 2C**).

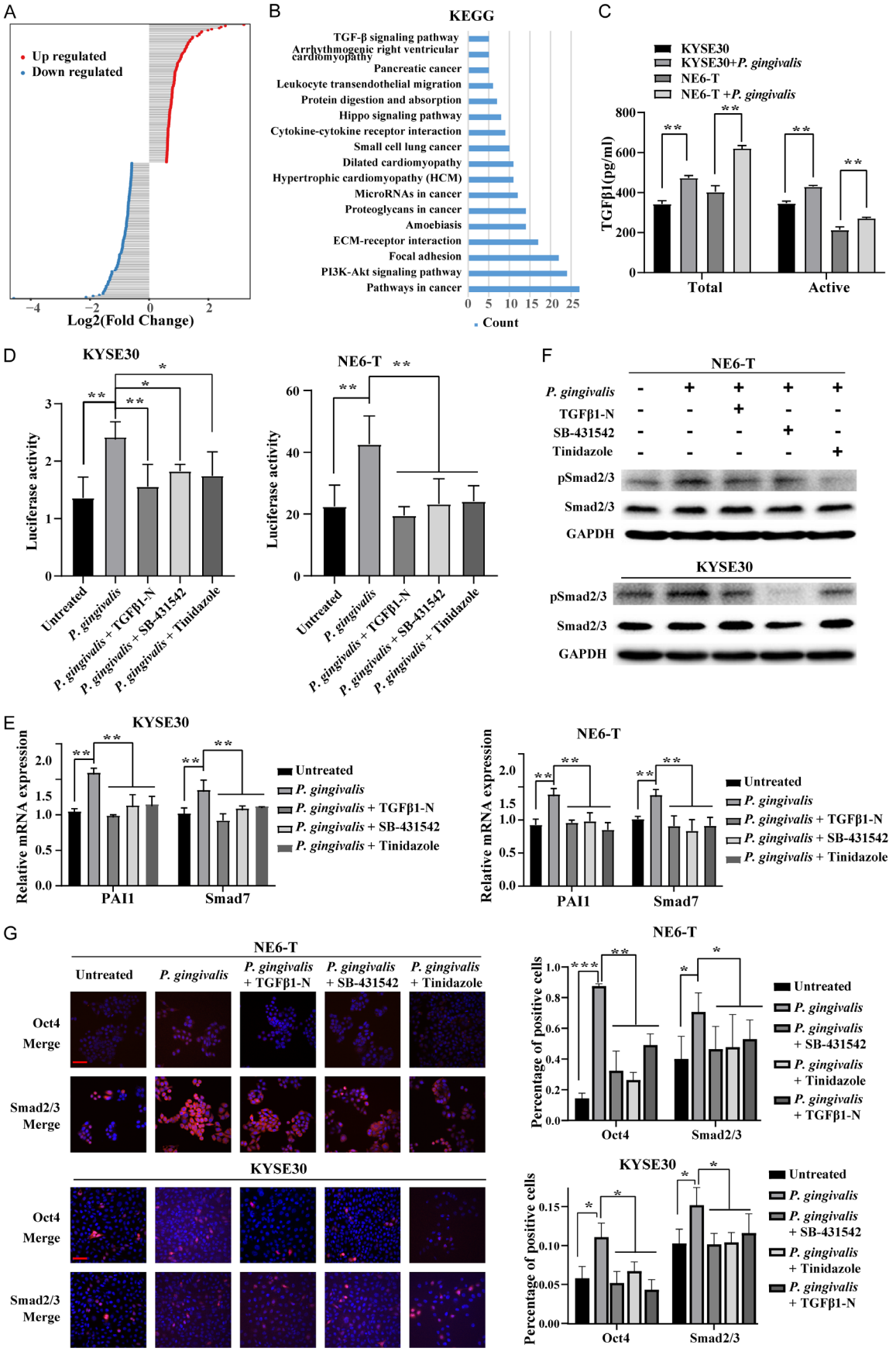
A
Up regulated
Down regulated
Log2(Fold Change)
B
KEGG
TGF-β signaling pathway
Arrhythmogenic right ventricular cardiomyopathy
Pancreatic cancer
Leukocyte transendothelial migration
Protein digestion and absorption
Hippo signaling pathway
Cytokine-cytokine receptor interaction
Small cell lung cancer
Dilated cardiomyopathy
Hypertrophic cardiomyopathy (HCM)
MicroRNAs in cancer
Proteoglycans in cancer
Amoebiasis
ECM-receptor interaction
Focal adhesion
PI3K-Akt signaling pathway
Pathways in cancer
Count
C
KYSE30
KYSE30+P. gingivalis
NE6-T
NE6-T +P. gingivalis
TGFβ1(pg/ml)
Total
Active
D
KYSE30
NE6-T
Luciferase activity
Untreated
P. gingivalis
P. gingivalis + TGFβ1-N
P. gingivalis + SB-431542
P. gingivalis + Tinidazole
F
NE6-T
P. gingivalis
TGFβ1-N
SB-431542
Tinidazole
pSmad2/3
Smad2/3
GAPDH
KYSE30
E
KYSE30
NE6-T
Relative mRNA expression
PAI1
Smad7
Untreated
P. gingivalis
P. gingivalis + TGFβ1-N
P. gingivalis + SB-431542
P. gingivalis + Tinidazole
G
NE6-T
Untreated
P. gingivalis
P. gingivalis + TGFβ1-N
P. gingivalis + SB-431542
P. gingivalis + Tinidazole
Oct4
Merge
Smad2/3
Merge
KYSE30
Percentage of positive cells
Oct4
Smad2/3

Figure 1. *P. gingivalis* infection upregulates TGFβ activity in ESCC. (A) Histogram showing the differentially expressed mRNAs in KYSE30 cells in response to *P. gingivalis* challenge; (B) Pathway enrichment analyses of differentially expressed mRNAs based on Kyoto Encyclopedia of Genes and Genomes (KEGG) database; (C) The expression levels of total and active TGFβ1 secreted by NE6-T and KYSE30 cells under different treatment conditions were detected by ELISA; (D) The activity of a TGFβ-responsive Smad-binding element (SBE) luciferase reporter in NE6-T or KYSE30 cells 24 h post *P. gingivalis* infection; (E) Plasminogen activator inhibitor-1 (PAI-1) and Smad7 mRNA expression levels in NE6-T and KYSE30 cells under different treatment conditions as determined by Real-time PCR; (F) The expression levels of pSmad2/3 and total Smad2/3 in NE6-T and KYSE30 cells under different treatment conditions as determined by Western blot; (G) Representative confocal immunofluorescence images and quantitation of Oct4 and Smad2/3 in NE6-T and KYSE30 cells under different treatment conditions. Scale bars, 50 μm. Except (A and B), all experiments were independently repeated three times. The quantitation data in (C-E) were presented as means ± SD from three independent experiment with a two-tailed Student's *t*-test for statistical analysis (**P* < 0.05, ***P* < 0.01, and ****P* < 0.001).

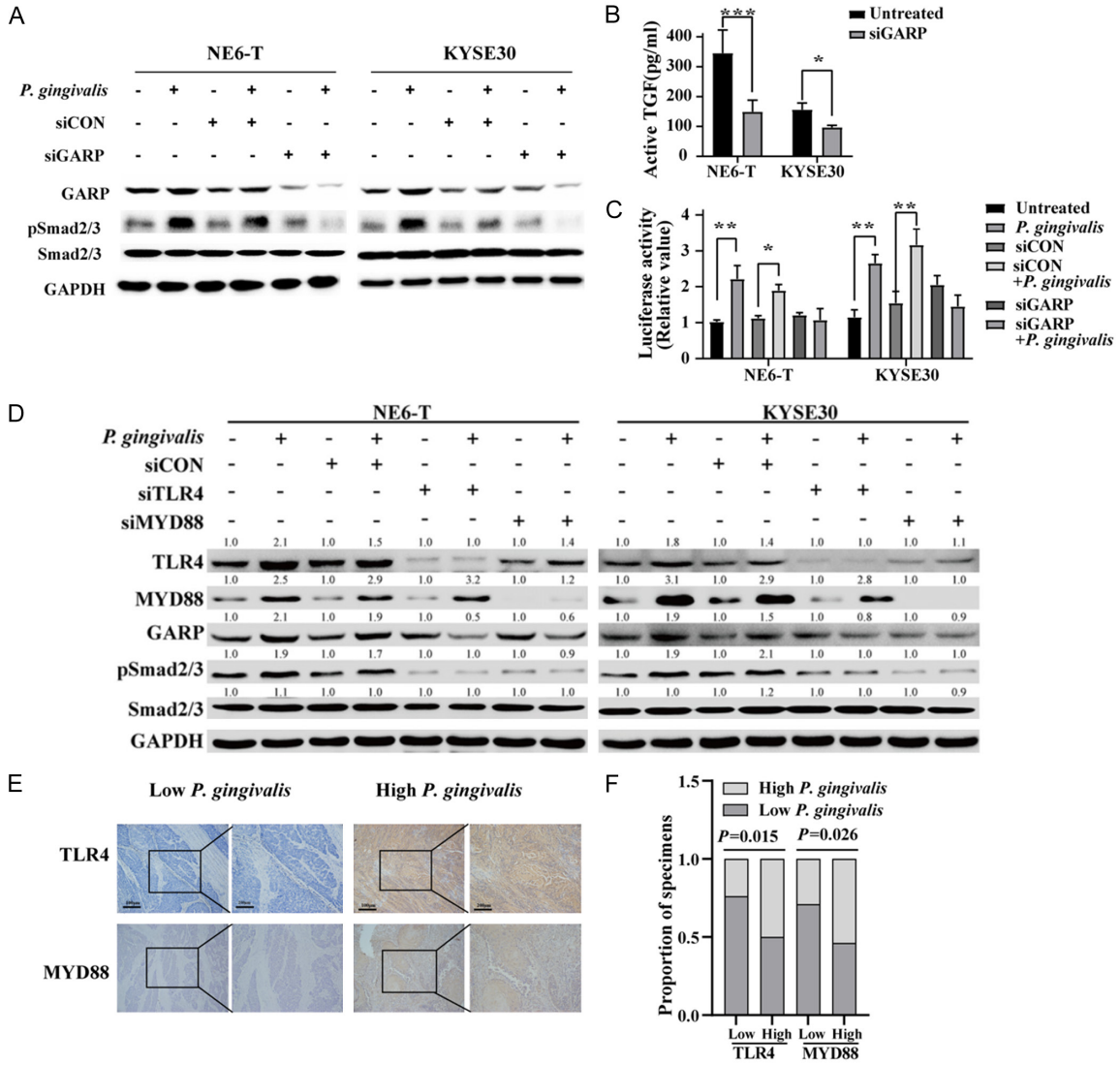

Figure 2. *P. gingivalis*-mediated upregulation of GARP enhances TGFβ activation through TLR4/MYD88 signaling. (A) The expression levels of indicated proteins in NE6-T and KYSE30 cells under different treatment conditions as determined by Western blot; (B) The expression level of active TGFβ secreted from NE6-T and KYSE30 cells in response to *P. gingivalis* was detected by ELISA; (C) The activity of a TGFβ-responsive Smad-binding element (SBE) luciferase reporter in GARP knockdown NE6-T and KYSE30 cells in response to *P. gingivalis* infection; (D) The expression levels of indicated proteins in NE6-T and KYSE30 cells under different treatment conditions as determined by Western blot. All experiments were independently repeated three times. (E) Representative images of IHC staining of TLR4 and MYD88 in tumor samples from ESCC patients with high- or low-levels of *P. gingivalis*. Scale bars, 200 μm and

100 μm, respectively. (F) Correlations between *P. gingivalis* and TLR4 protein, as well as between *P. gingivalis* and MYD88 protein. The quantitation data in (B and C) were presented as means ± SD from three independent experiment with a two-tailed Student's *t*-test for statistical analysis. The Spearman nonparametric correlation test was employed to analyze the correlations among the ranked factors in (F) (**P* < 0.05, ***P* < 0.01, and ****P* < 0.001).

Taken together, these results strongly suggested that *P. gingivalis* infection-induced upregulation of GAPR mediated the enhancement of TGFβ signaling in ESCC cells.

Furthermore, we investigated how *P. gingivalis* infection upregulates GAPR in ESCC cells. Similar to recent reports that *Fusobacterium nucleatum*, a gram-negative anaerobe, can activate the toll-like receptor 4 (TLR4)/MyD88 cascade, thereby promoting the progression and chemoresistance of colorectal cancer [4, 38], we found that *P. gingivalis* infection resulted in an upregulation of TLR4 and MyD88 protein levels in ESCC cells (**Figure 2D**), suggesting that the TLR4/MyD88 pathway might mediate the activity of *P. gingivalis*. In support with this notion, knockdown of TLR4 or MyD88 markedly reduced the upregulation of GARP and the enhanced Smad2/3 activity by *P. gingivalis* (**Figure 2D**). In addition, the protein levels of TLR4 and MyD88 were significantly higher in *P. gingivalis*-infected samples than in the non-infected controls from ESCC xenograft tumors and ESCC patients (**Figures 2E**, **2F** and S1). These findings demonstrated the involvement of TLR4/MyD88 in the upregulation of GARP. Collectively, our results revealed that *P. gingivalis* activates the TGFβ signaling pathway through GARP via the upregulation of TLR4/MyD88, at least partially, in ESCC cells.

pSmad2/3 was negatively associated with overall survival in ESCC patients

Our previous studies reported that *P. gingivalis* abundance in ESCC was significantly correlated with a shorter survival of ESCC patients [3, 12]. Since we observed that *P. gingivalis* infection activated TGFβ signaling in this study, we queried the clinical significance of this activation in the overall survival of ESCC patients. As shown in **Figure 3A-C**, the protein levels of GARP, pSmad2, and TGFβ1 were significantly increased in *P. gingivalis*-high ESCC tissues, and more importantly, these protein levels were positively correlated with the abundance of *P. gingivalis*. There was also a significant correlation between GARP and pSmad2/3 level (**Figure 3C**). Further analysis showed that the high level of pSmad2 was significantly associated with the poor overall survival of ESCC patients (**Figure 3D**), while only a marginal correlation between GARP level and the overall survival was detected (**Figure 3E**). Surprisingly, there was no correlation between TGFβ1 level and the overall survival (**Figure 3F**), which might be because IHC staining used to detect TGFβ1 in cancer tissues was not sensitive enough to accurately reflect the expression of various forms of TGFβ1. Alternatively, other signaling pathways might modulate TGFβ1 activity in ESCC. Nevertheless, our results suggest that *P. gingivalis*-mediated GARP upregulation was related to the poor overall survival of ESCC patients through the activation of TGFβ/Smad2/3 signaling.

The pro-tumorigenic property of P. gingivalis was dependent on the intactness of fimbriae

P. gingivalis fimbriae are proteinaceous, filamentous appendages that protrude from the bacterial cell surface [39]. The fimbriae of *P. gingivalis* play crucial roles in biofilm formation, auto-aggregation and co-aggregation with other oral bacteria, adhesion to host molecules, and host cell invasion [39-41]. For example, it has been reported that a *P. gingivalis* Δ*fimA* mutant loses its ability to invade epithelial cells [42, 43]. Hence, we evaluated if FimA was required for *P. gingivalis* to activate TGFβ signaling by using the *fimA* deletion mutant of *P. gingivalis*. As shown in **Figure 4A**, the *fimA* mutant exhibited a diminished ability to activate TGFβ signaling in KYSE30 and NE6-T cells. Notably, the *fimA* mutant demonstrated reduced internalization as well as suppressed abilities to promote cellular proliferation, migration, and invasion compared to the wild-type *P. gingivalis* control (**Figure 4B-D**), indicating that FimA contributed partly to the tumor-promoting role of *P. gingivalis* through TGFβ/Smad signaling.

In addition to its role in regulating TGFβ signaling, we also found that *P. gingivalis* upregulated the expression of cell cycle inhibitors and apop-

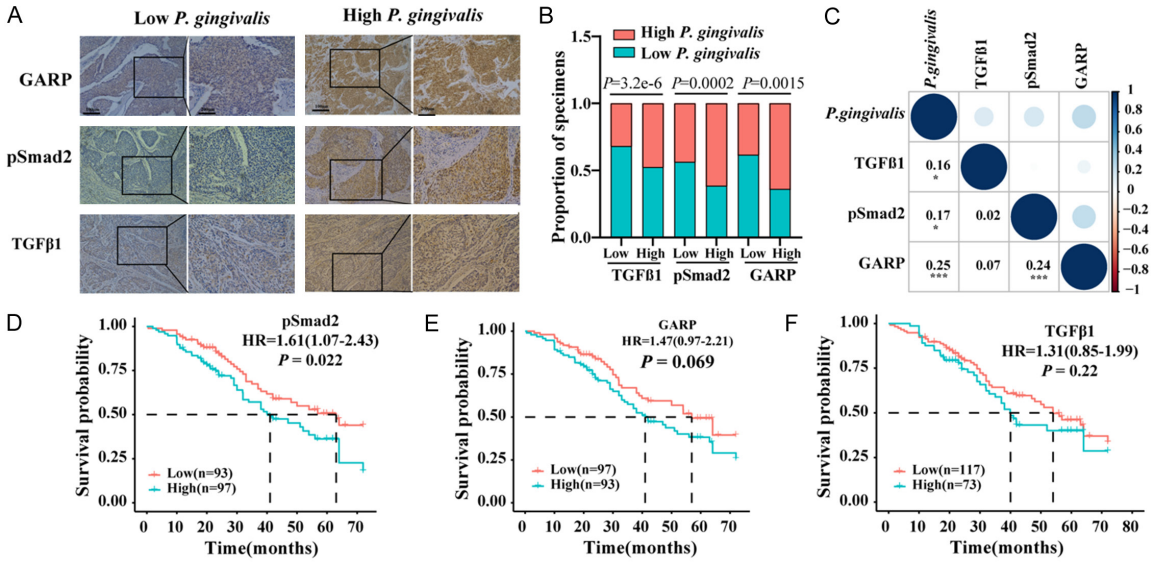

Figure 3. pSmad2 level was positively associated with unfavorable overall survival in ESCC patients. (A) Representative images of IHC staining of GARP and pSmad2 in ESCC with high- or low-levels of *P. gingivalis*. Scale bars, 200 μm and 100 μm, respectively; (B, C) Correlations between *P. gingivalis* and GARP, *P. gingivalis* and pSmad2, as well as *P. gingivalis* and TGFβ1; (D-F) Kaplan-Meier analyses on the overall survival of ESCC patients with low- and high-levels of GARP, pSmad2, and TGFβ1. The Spearman nonparametric correlation test was employed to analyze the correlations among the ranked factors in (B and C).

tosis-related genes such as CDKN2B and BMF (**Figure 4E**). Furthermore, since TGFβ signaling controls epithelial-mesenchymal transition (EMT), cancer cell stemness, tumor cell growth, and migration [6, 13], we examined the effect of *P. gingivalis* infection on the marker gene expression of these pathways in NE6-T and KYSE30 cells and found that *P. gingivalis* infection downregulated the expression of E-cadherin, while upregulated the expression of N-cadherin and EMT inducer Snail (**Figure 4F**). Similarly, both western blotting and IF staining demonstrated that *P. gingivalis* increased the expression of pluripotency marker Oct4, and importantly, all these properties were abolished by TGFβ1-N, SB-431542, or tinidazole pretreatment (**Figures 4F**, **1G**). Moreover, Western blotting showed that GARP depletion abrogated *P. gingivalis*-induced pSmad2/3, PAI-1, Snail, and Oct4 levels (**Figure 4G**), suggesting the essential role of GARP in *P. gingivalis*-induced effects. Importantly, the *P. gingivalis*-induced malignant phenotypes, such as enhanced migration and invasion, were abolished by TGFβ1-N, SB-431542, or tinidazole pretreatment (Figure S2A). Likewise, GARP knockdown also hampered *P. gingivalis*-induced migration and invasion of ESCC cell (Figure S2B). Taken together, these results suggest that *P. gingivalis* aggravates ESCC possibly through a fimbriae-dependent TGFβ activation, and at least partially, rewires other pro-oncogenic signaling pathways including pro-EMT and cancer stemness in ESCC cells.

Elimination of P. gingivalis or inhibition of TGFβ signaling suppressed the growth and metastasis of ESCC in mouse models

To confirm our findings from in vitro cell line-based studies, we examined the effects of inhibiting TGFβ signaling and/or eliminating *P. gingivalis* on the growth and metastasis of ESCC in mouse models. Specifically, *P. gingivalis*-treated or untreated NE6-T cells were subcutaneously inoculated in nude mice, followed by the treatment with SB-431542 or tinidazole. We found that *P. gingivalis* infection significantly augmented tumor growth, which could be significantly reduced by SB-431542. Interestingly, tinidazole treatment rendered a similar inhibitory effect (**Figure 5A**). Furthermore, real-time PCR analyses of xenograft tumors showed that *P. gingivalis* upregulated the mRNA levels of PAI-1, Smad7, Snail, and Oct4, which could be attenuated by SB-431542 or tinidazole, except for Smad7 (**Figure 5B**). A similar effect was also observed on the protein levels of pSmad2, PAI-

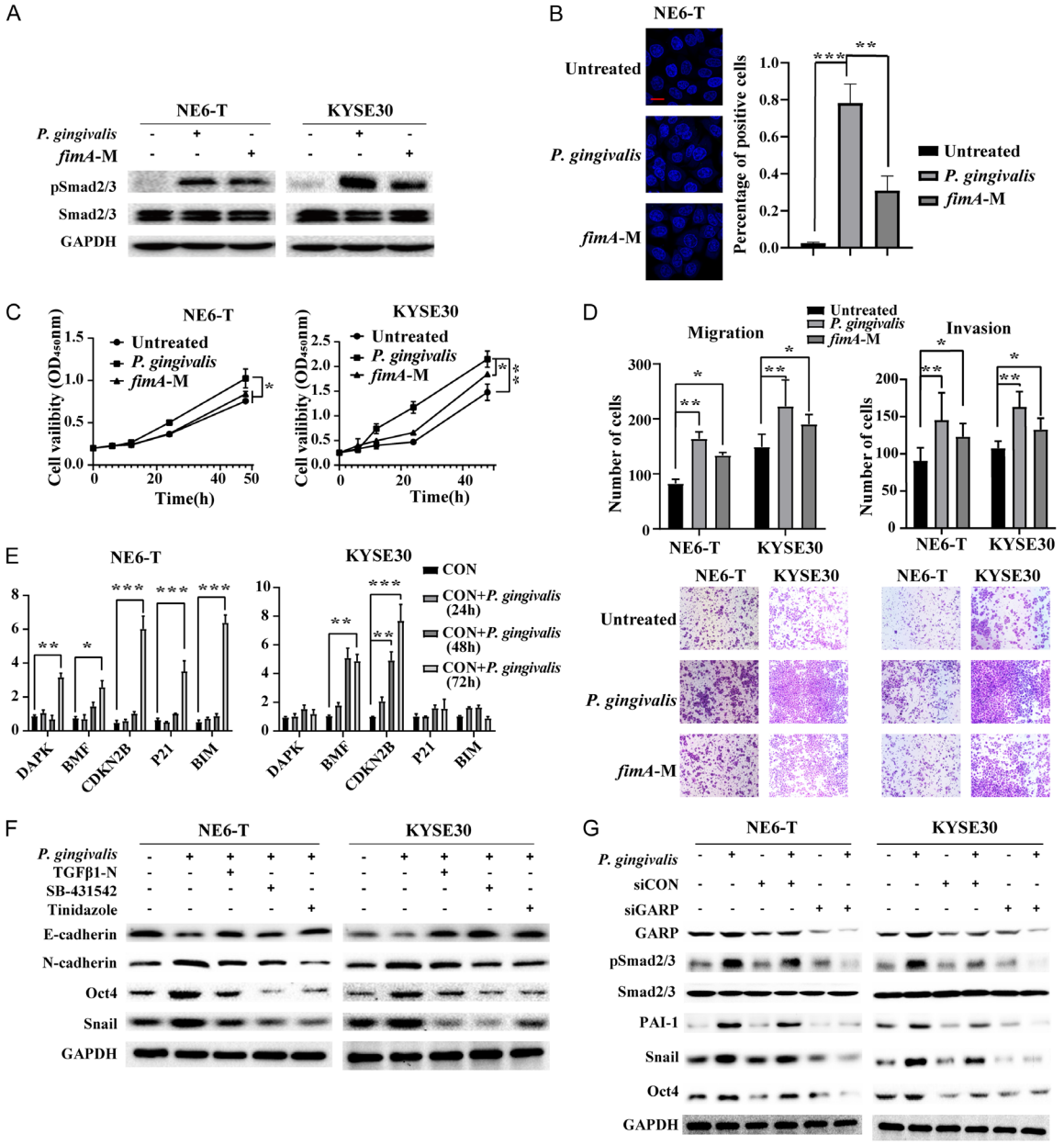

Figure 4. Fimbriae and GARP were required for *P. gingivalis*-activated TGFβ signaling. (A) The expression levels of indicated proteins in NE6-T and KYSE30 cells in response to *P. gingivalis* or a *fimA* deficient mutant (*fimA*-M) treatment as determined by Western blot; (B) Representative confocal immunofluorescence images and the quantitation of the intracellular invasion into NE6-T cells by *P. gingivalis or fimA*-M *P. gingivalis*. Scale bar, 50 μm; (C) Cell viability was measured by MTT assay in NE6-T and KYSE30 cells in response to *P. gingivalis or fimA*-M; (D) Representative images as well as the quantitation of the migration and invasion of NE6-T and KYSE30 cells in response to *P. gingivalis or fimA*-M; (E) The mRNA expression levels of cell cycle inhibitors and apoptosis-related genes in NE6-T and KYSE30 cells under different treatment conditions as determined by real-time PCR; (F, G) The expression levels of indicated proteins in NE6-T and KYSE30 cells in response to *P. gingivalis* under different treatment conditions as determined by Western blot. All experiments were independently repeated three times. The quantitation data in (B-D) were presented as means ± SD from three independent experiment with a two-tailed Student's *t*-test for statistical analysis (**P* < 0.05, ***P* < 0.01, and ****P* < 0.001).

1, Snail, and Oct4 by IHC (**Figure 5C**). Consistent with these data, active TGFβ level was significantly enhanced in the xenograft tumors derived from *P. gingivalis*-treated ESCC cells (**Figure 5D**). In addition, lung bioluminescence analysis of the tail vein injected mice revealed that *P. gingivalis* infection promoted tumor growth and lung metastasis, which could be

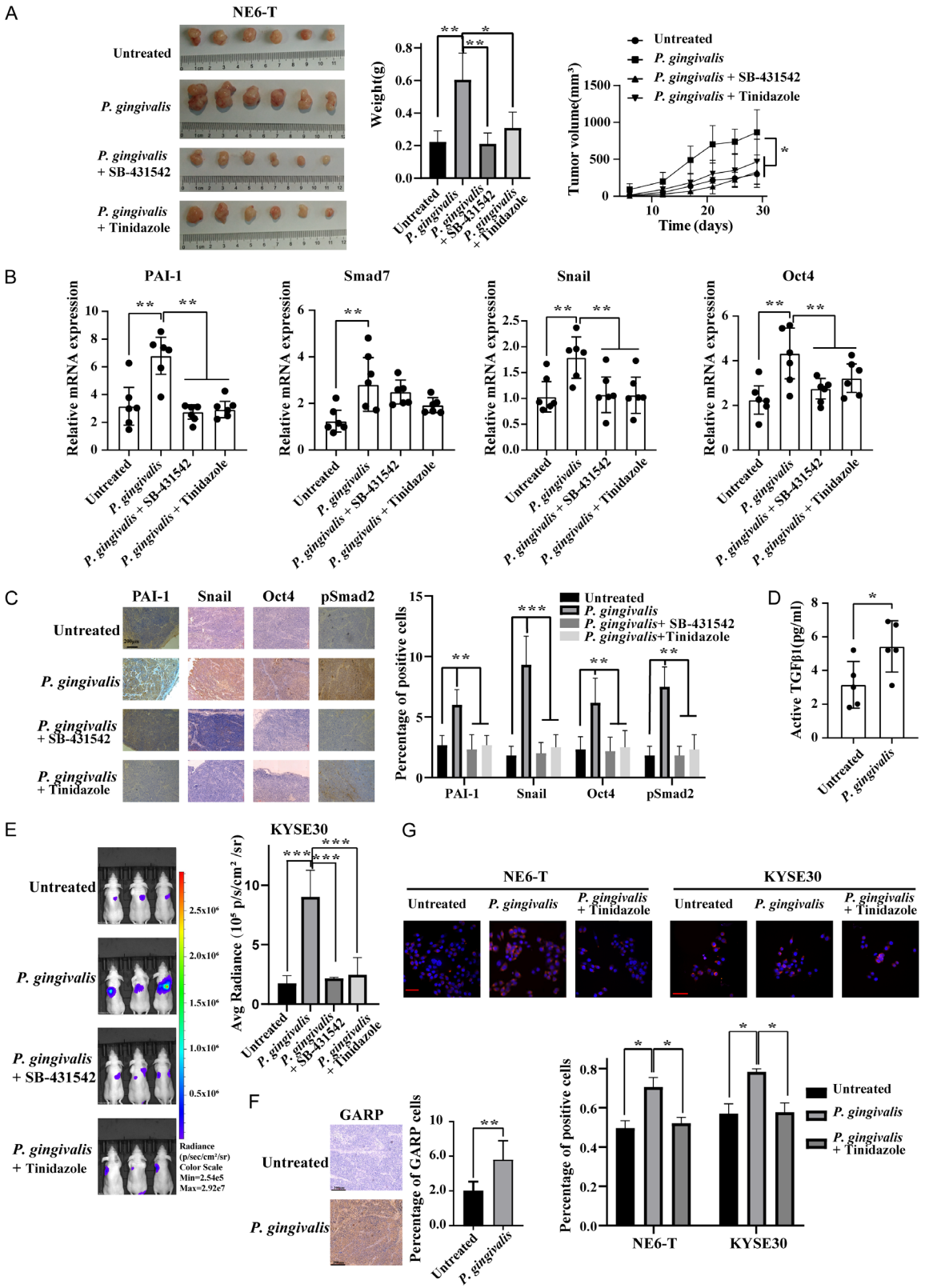

Figure 5. Eliminating *P. gingivalis* or inhibiting TGFβ signaling suppressed ESCC tumor growth and metastasis in mouse xenograft models. (A) Representative images and quantitation of the weight and volume of NE6-T cells-derived xenograft tumor pretreated with *P. gingivalis* or PBS; (B) The mRNA levels of indicated molecules in NE6-T-derived xenografted tumors under different treatment conditions as determined by real-time PCR; (C) IHC staining of

pSmad2, PAI-1, Snail, and Oct4 in NE6-T-derived xenograft tumors under different treatment conditions. Scale bars, 200 μm. (D) The expression of level of active TGFβ in NE6-T-derived xenograft tumors in response to *P. gingivalis* was measured by ELISA; (E) Representative bioluminescent images of photon flux and quantification of photon flux of lung metastasis from tail vein injection of KYSE30 cells under different treatment conditions; (F) IHC staining of GARP in NE6-T-derived xenograft tumors in response to *P. gingivalis*. Scale bars, 200 μm; (G) Representative confocal immunofluorescence images and the quantitation of GARP in NE6-T and KYSE30 cells under different treatment conditions. Scale bars, 50 μm. Except (C and F), all experiments were independently repeated three times. Except (G), the quantitation data were presented as means ± SD from three independent experiment with a two-tailed two-way ANOVA test, Student's *t*-test, or nonparametric Mann-Whitney test for statistical analyses (**P* < 0.05, ***P* < 0.01, and ****P* < 0.001).

attenuated by inhibitors (**Figure 5E**). Lastly, IF staining demonstrated a higher expression level of GARP in *P. gingivalis*-infected cells-derived xenograft tumors (**Figure 5F**). Notably, *P. gingivalis* induced a predominantly membranous and para-membranous distribution of GARP in ESCC cells, which would facilitate the enrichment of TGFβ signaling (**Figure 5G**).

Discussion

Aberrant TGFβ signaling is well known to be involved in the progression of multiple cancers in a context-dependent manner. However, the role and functional mechanism of this signaling in the infectious milieu of ESCC remain largely unknown. In this study, we demonstrated for the first time that *P. gingivalis* infection promoted TGFβ signaling and subsequently worsened the prognosis of ESCC patients. Furthermore, we found that *P. gingivalis*-induced TGFβ activation was mediated by the upregulation of a surface receptor, GARP, which subsequently activated multiple downstream signaling molecules as well as EMT and cancer cell stemness. In addition, we found that the FimA fimbriae of *P. gingivalis* signaling through TLR4/MyD88 was required for the upregulation of GARP. Collectively, our findings demonstrated the protumorigenic property of *P. gingivalis* through the upregulation of TGFβ signaling, as well as a novel regulatory mechanism mediated by GARP in the activation of the TGFβ signaling in ESCC.

Our results showed that the upregulation of GARP by *P. gingivalis* was dependent on fimbrial production and the activation of TLR4/MyD88 in ESCC cells. These findings not only revealed that GARP was the target of *P. gingivalis* but also elucidated the underlying molecular mechanisms of *P. gingivalis*-induced TGFβ signaling. This function of *P. gingivalis* is specific as challenging with *E. coli,* a classic bacterium that produces the agonist of TLR4-signaling *in vivo*, fails to enhance GARP (data not shown), suggesting that other virulence factor(s) of *P. gingivalis* might also be involved in the upregulation of GARP. In addition, it is well known that a high level of latent TGFβ is sequestered in the extracellular matrix of tumor or in other cells, where latent TGFβ is activated by protease cleavage, such as MMP-2 and MMP-9, thereby releasing the active form of TGFβ into the tumor microenvironment [44-46]. Alternatively, since *P. gingivalis* infection can consistently elevate the secretion of MMPs in different contexts [47-50], the increased MMPs in the tumor microenvironment may lead to the elevated TGFβ activity and enhanced malignancy of ESCC. Our results from this study showed that the upregulation of GARP and TLR4/MyD88 was required for TGFβ activation, suggesting that *P. gingivalis* employed at least three distinct strategies to activate TGFβ signaling: the secretion of MMPs, the activation of TLR4/MyD88, and the upregulation of GAPR expression. Further investigation on the secretion of active TGFβ will provide insight into the pro-tumorigenic mechanism of *P. gingivalis* infection in ESCC.

Previous studies have reported an increased TGFβ level in the serum of ESCC patients, which was associated with shorter survival time of the patients [51], suggesting that TGFβ level could be a prognostic marker for ESCC. Since the phosphorylation of Smad2 and Smad3 is the central event in TGFβ signaling [52, 53], we examined the pSmad2/3 level in *P. gingivalis*-infected ESCC cells as well as in the tumor tissues from patients and found remarkably increased pSmad2/3 levels, suggesting that increased Smad2/3 phosphorylation could be used as a prognostic marker in ESCC. However, an opposite conclusion was drawn from a recent meta-analysis, in which lower pSmad2 level was significantly associated with an increased all-cause mortality risk in cancer patients [54]. In addition, there are several

studies showing pSmad2 [55-59] and pSmad3 [60, 61] could be either an adverse effecter or a favorable effecter in different types, or even the same type of tumors, which could be due to the specific cancer type used in different studies or the non-overlapping, opposite function of pSmad2 and pSmad3 during tumor progression [53, 62, 63].

Other regulatory proteins are also involved in regulating TGFβ activity in the tumor microenvironment. For example, Smad ubiquitination regulatory factor (Smurf)-mediated TβRI degradation can dynamically regulate TGFβ signaling [64]. As recent studies have shown that *P. gingivalis* is a potent inducer of several ubiquitin E3 ligases [65, 66], it is conceivable that ubiquitination-mediated degradation of SMAD could be exploited by *P. gingivalis* to aggravate ESSC. Indeed, a previous study showed a significant increase of Smurf in ESCC tissues [67]. In this study, we found that the phosphorylation of Smad2/3 and Smad7 were increased in *P. gingivalis*-stimulated ESCC cells. Since previous studies have indicated that the inhibitory Smad protein Smad7 can bind to TGF-β receptors and interfere with the phosphorylation of Smad2/3 [68, 69], we therefore cannot exclude the possibility that Smad7 regulated the abundance of Smad2/3 in ESCC. Furthermore, it has been reported Smad7 expression is increased in response to the proinflammatory cytokines such as interferon-γ (IFN-γ) and TNFα, which activate the JAK/STAT and NF-κB signaling pathway, respectively, in some cell types [70]. Since *P. gingivalis* infection increases the proinflammatory cytokine production by innate cells in the infectious tumor microenvironments, these findings suggest the importance of the window of time in which TGFβ and SMADs proteins should be examined. Therefore, a detailed examination on the phosphorylation and total SMAD levels in patient tissues would be necessary to define the role of TGFβ and its downstream signaling components in the progression of ESCC.

While this study found that *P. gingivalis* promoted TGFβ secretion and activation, we cannot exclude the possibility that other bacteria in the oral cavity may also affect TGFβ expression and its downstream signaling through altering the growth of *P. gingivalis* and/or the composition of the local microbiome in the infectious milieu. Previous studies have reported that the delivery of some commensal bacteria or the infection of *Fusobacterium nucleatum* are indeed associated with the higher expression of TGFβ [71, 72]. Considering the *de facto* status of the colonization of various bacterial species in esophageal microenvironment [10, 73], the indirect impact of other oral microbes on TGFβ expression should be investigated to characterize the influence of *P. gingivalis* and other bacteria, alone and in combination, on the expression of TGFβ and the prognosis of ESCC.

In this study, we found that the administration of tinidazole, an antibiotic targeting *P. gingivalis,* led to a significantly decreased tumor growth. Further characterization revealed that tinidazole treatment inhibited TGFβ activity as well as the expression of GARP, pSMAD2/3, and other signaling molecules, suggesting the potential application of targeting *P. gingivalis* infection in ESCC therapy. However, caution should be taken to advocate the use of tinidazole since tinidazole targets a group of anaerobic bacteria including those interacted with *P. gingivalis*; hence, the development of a *P. gingivalis*-specific antimicrobial agent such as protein peptide with specific motifs to neutralize the binding or invasion of *P. gingivalis* may be required. Additionally, further studies on the effect of tinidazole on cancer cell immune evasion and the related pathogenesis are required to comprehensively assess the influence of antibiotics on the progression and prognosis of ESCC.

In conclusion, we have demonstrated for the first time that *P. gingivalis* infection enhanced TGFβ signaling in cultured ESCC cells and in xenograft tumor. Furthermore, we found that the *P. gingivalis* infection-mediated increase of GARP and the subsequent MyD88 signaling were required for the phosphorylation of SMADs. Moreover, our clinical data showed that *P. gingivalis* infection and the phosphorylation of Smad2/3 were significantly associated with the overall survival of patients with ESCC. More importantly, inhibiting TGFβ signaling or eliminating *P. gingivalis* suppressed tumor growth and metastasis, suggesting the potential clinical application of targeting *P. gingivalis*-related signaling network for the treatment of patients with ESCC.

Acknowledgements

This project was supported in part by grants from the National Natural Science Foundation

of China (81872037, U1604191, 81472234), Scientific and Technological Innovation Team of Higher Education of Henan (15IRTSTHN024), Henan Science and Technology Major Project (161100311200), Key R&D and Promotion Projects of Henan Province (222102310115), and Key Projects of Medical Science and Technology of Henan Province (SBGJ20210-2199).

Disclosure of conflict of interest

None.

Address correspondence to: Shegan Gao and Yi-Jun Qi, State Key Laboratory of Esophageal Cancer Prevention & Treatment, Henan Key Laboratory of Microbiome and Esophageal Cancer Prevention and Treatment, Henan Key Laboratory of Cancer Epigenetics, Cancer Hospital, The First Affiliated Hospital, College of Clinical Medicine, Medical College of Henan University of Science and Technology, Luoyang 471003, Henan, China. Tel: +86-379-69823137; Fax: +86-379-64820811; E-mail: gsg112258@163.com (SGG); qiyijun@haust.edu.cn (YJQ)

References

[1] Jin C, Lagoudas GK, Zhao C, Bullman S, Bhutkar A, Hu B, Ameh S, Sandel D, Liang XS, Mazzilli S, Whary MT, Meyerson M, Germain R, Blainey PC, Fox JG and Jacks T. Commensal microbiota promote lung cancer development via gammadelta T cells. Cell 2019; 176: 998-1013, e1016.

[2] Tjalsma H, Boleij A, Marchesi JR and Dutilh BE. A bacterial driver-passenger model for colorectal cancer: beyond the usual suspects. Nat Rev Microbiol 2012; 10: 575-582.

[3] Gao S, Liu Y, Duan X, Liu K, Mohammed M, Gu Z, Ren J, Yakoumatos L, Yuan X, Lu L, Liang S, Li J, Scott DA, Lamont RJ, Zhou F and Wang H. Porphyromonas gingivalis infection exacerbates oesophageal cancer and promotes resistance to neoadjuvant chemotherapy. Br J Cancer 2021; 125: 433-444.

[4] Yu T, Guo F, Yu Y, Sun T, Ma D, Han J, Qian Y, Kryczek I, Sun D, Nagarsheth N, Chen Y, Chen H, Hong J, Zou W and Fang JY. Fusobacterium nucleatum promotes chemoresistance to colorectal cancer by modulating autophagy. Cell 2017; 170: 548-563, e516.

[5] Bullman S, Pedamallu CS, Sicinska E, Clancy TE, Zhang X, Cai D, Neuberg D, Huang K, Guevara F, Nelson T, Chipashvili O, Hagan T, Walker M, Ramachandran A, Diosdado B, Serna G, Mulet N, Landolfi S, Ramon Y Cajal S, Fasani R, Aguirre AJ, Ng K, Elez E, Ogino S, Tabernero J, Fuchs CS, Hahn WC, Nuciforo P and Meyerson M. Analysis of fusobacterium persistence and antibiotic response in colorectal cancer. Science 2017; 358: 1443-1448.

[6] Ohshima J, Wang Q, Fitzsimonds ZR, Miller DP, Sztukowska MN, Jung YJ, Hayashi M, Whiteley M and Lamont RJ. Streptococcus gordonii programs epithelial cells to resist ZEB2 induction by Porphyromonas gingivalis. Proc Natl Acad Sci U S A 2019; 116: 8544-8553.

[7] Zagato E, Pozzi C, Bertocchi A, Schioppa T, Saccheri F, Guglietta S, Fosso B, Melocchi L, Nizzoli G, Troisi J, Marzano M, Oresta B, Spadoni I, Atarashi K, Carloni S, Arioli S, Fornasa G, Asnicar F, Segata N, Guglielmetti S, Honda K, Pesole G, Vermi W, Penna G and Rescigno M. Endogenous murine microbiota member Faecalibaculum rodentium and its human homologue protect from intestinal tumour growth. Nat Microbiol 2020; 5: 511-524.

[8] Lamont RJ, Fitzsimonds ZR, Wang H and Gao S. Role of Porphyromonas gingivalis in oral and orodigestive squamous cell carcinoma. Periodontol 2000 2022; 89: 154-165.

[9] Geller LT, Barzily-Rokni M, Danino T, Jonas OH, Shental N, Nejman D, Gavert N, Zwang Y, Cooper ZA, Shee K, Thaiss CA, Reuben A, Livny J, Avraham R, Frederick DT, Ligorio M, Chatman K, Johnston SE, Mosher CM, Brandis A, Fuks G, Gurbatri C, Gopalakrishnan V, Kim M, Hurd MW, Katz M, Fleming J, Maitra A, Smith DA, Skalak M, Bu J, Michaud M, Trauger SA, Barshack I, Golan T, Sandbank J, Flaherty KT, Mandinova A, Garrett WS, Thayer SP, Ferrone CR, Huttenhower C, Bhatia SN, Gevers D, Wargo JA, Golub TR and Straussman R. Potential role of intratumor bacteria in mediating tumor resistance to the chemotherapeutic drug gemcitabine. Science 2017; 357: 1156-1160.

[10] Yuan X, Liu Y, Kong J, Gu B, Qi Y, Wang X, Sun M, Chen P, Sun W, Wang H, Zhou F and Gao S. Different frequencies of Porphyromonas gingivalis infection in cancers of the upper digestive tract. Cancer Lett 2017; 404: 1-7.

[11] Wang X, Jia Y, Wen L, Mu W, Wu X, Liu T, Liu X, Fang J, Luan Y, Chen P, Gao J, Nguyen KA, Cui J, Zeng G, Lan P, Chen Q, Cheng B and Wang Z. Porphyromonas gingivalis promotes colorectal carcinoma by activating the hematopoietic nlrp3 inflammasome. Cancer Res 2021; 81: 2745-2759.

[12] Gao S, Li S, Ma Z, Liang S, Shan T, Zhang M, Zhu X, Zhang P, Liu G, Zhou F, Yuan X, Jia R, Potempa J, Scott DA, Lamont RJ, Wang H and Feng X. Presence of porphyromonas gingivalis in esophagus and its association with the clinicopathological characteristics and survival in

patients with esophageal cancer. Infect Agent Cancer 2016; 11: 3.
[13] Ha NH, Woo BH, Kim DJ, Ha ES, Choi JI, Kim SJ, Park BS, Lee JH and Park HR. Prolonged and repetitive exposure to Porphyromonas gingivalis increases aggressiveness of oral cancer cells by promoting acquisition of cancer stem cell properties. Tumour Biol 2015; 36: 9947-9960.
[14] Ren J, Han X, Lohner H, Hoyle RG, Li J, Liang S and Wang H. P. gingivalis infection upregulates PD-L1 expression on dendritic cells, suppresses CD8+ T-cell responses, and aggravates oral cancer. Cancer Immunol Res 2023; 11: 290-305.
[15] Ren J, Han X, Lohner H, Liang R, Liang S and Wang H. Serum- and glucocorticoid-inducible kinase 1 promotes alternative macrophage polarization and restrains inflammation through FoxO1 and STAT3 signaling. J Immunol 2021; 207: 268-280.
[16] Laiho M, Weis FM, Boyd FT, Ignotz RA and Massague J. Responsiveness to transforming growth factor-beta (TGF-beta) restored by genetic complementation between cells defective in TGF-beta receptors I and II. J Biol Chem 1991; 266: 9108-9112.
[17] Zuniga JE, Groppe JC, Cui Y, Hinck CS, Contreras-Shannon V, Pakhomova ON, Yang J, Tang Y, Mendoza V, Lopez-Casillas F, Sun L and Hinck AP. Assembly of TbetaRI:TbetaRII:TGFβeta ternary complex in vitro with receptor extracellular domains is cooperative and isoform-dependent. J Mol Biol 2005; 354: 1052-1068.
[18] Feng XH and Derynck R. Specificity and versatility in tgf-beta signaling through Smads. Annu Rev Cell Dev Biol 2005; 21: 659-693.
[19] Massague J. How cells read TGF-beta signals. Nat Rev Mol Cell Biol 2000; 1: 169-178.
[20] Hill CS. Transcriptional control by the SMADs. Cold Spring Harb Perspect Biol 2016; 8: a022079.
[21] David CJ and Massague J. Contextual determinants of TGFβeta action in development, immunity and cancer. Nat Rev Mol Cell Biol 2018; 19: 419-435.
[22] Derynck R, Akhurst RJ and Balmain A. TGF-beta signaling in tumor suppression and cancer progression. Nat Genet 2001; 29: 117-129.
[23] Yang L and Moses HL. Transforming growth factor beta: tumor suppressor or promoter? Are host immune cells the answer? Cancer Res 2008; 68: 9107-9111.
[24] Buck MB, Fritz P, Dippon J, Zugmaier G and Knabbe C. Prognostic significance of transforming growth factor beta receptor II in estrogen receptor-negative breast cancer patients. Clin Cancer Res 2004; 10: 491-498.
[25] Friedman E, Gold LI, Klimstra D, Zeng ZS, Winawer S and Cohen A. High levels of transforming growth factor beta 1 correlate with disease progression in human colon cancer. Cancer Epidemiol Biomarkers Prev 1995; 4: 549-554.
[26] Katz LH, Likhter M, Jogunoori W, Belkin M, Ohshiro K and Mishra L. TGF-beta signaling in liver and gastrointestinal cancers. Cancer Lett 2016; 379: 166-172.
[27] Song W, Dai WJ, Zhang MH, Wang H and Yang XZ. Comprehensive analysis of the expression of TGF-beta signaling regulators and prognosis in human esophageal cancer. Comput Math Methods Med 2021; 2021: 1812227.
[28] Tsushima H, Kawata S, Tamura S, Ito N, Shirai Y, Kiso S, Imai Y, Shimomukai H, Nomura Y, Matsuda Y and Matsuzawa Y. High levels of transforming growth factor beta 1 in patients with colorectal cancer: association with disease progression. Gastroenterology 1996; 110: 375-382.
[29] Wu F, Weigel KJ, Zhou H and Wang XJ. Paradoxical roles of TGF-beta signaling in suppressing and promoting squamous cell carcinoma. Acta Biochim Biophys Sin (Shanghai) 2018; 50: 98-105.
[30] Li MO and Flavell RA. TGF-beta: a master of all T cell trades. Cell 2008; 134: 392-404.
[31] Tran DQ. TGF-beta: the sword, the wand, and the shield of FOXP3(+) regulatory T cells. J Mol Cell Biol 2012; 4: 29-37.
[32] Metelli A, Wu BX, Fugle CW, Rachidi S, Sun S, Zhang Y, Wu J, Tomlinson S, Howe PH, Yang Y, Garrett-Mayer E, Liu B and Li Z. Surface expression of TGFβeta docking receptor garp promotes oncogenesis and immune tolerance in breast cancer. Cancer Res 2016; 76: 7106-7117.
[33] Carrillo-Galvez AB, Quintero JE, Rodriguez R, Menendez ST, Victoria Gonzalez M, Blanco-Lorenzo V, Allonca E, de Araujo Farias V, Gonzalez-Correa JE, Erill-Sagales N, Martinez-Zubiaurre I, Hellevik T, Sanchez-Hernandez S, Munoz P, Zurita F, Martin F, Rodriguez-Manzaneque JC and Anderson P. GARP promotes the proliferation and therapeutic resistance of bone sarcoma cancer cells through the activation of TGF-beta. Cell Death Dis 2020; 11: 985.
[34] Hahn SA, Neuhoff A, Landsberg J, Schupp J, Eberts D, Leukel P, Bros M, Weilbaecher M, Schuppan D, Grabbe S, Tueting T, Lennerz V, Sommer C, Jonuleit H and Tuettenberg A. A key role of GARP in the immune suppressive tumor microenvironment. Oncotarget 2016; 7: 42996-43009.
[35] Jin H, Sun L, Tang L, Yu W and Li H. Expression of GARP Is increased in tumor-infiltrating regulatory T cells and is correlated to clinicopathol-

ogy of lung cancer patients. Front Immunol 2017; 8: 138.
[36] Salem M, Wallace C, Velegraki M, Li A, Ansa-Addo E, Metelli A, Kwon H, Riesenberg B, Wu B, Zhang Y, Guglietta S, Sun S, Liu B and Li Z. GARP dampens cancer immunity by sustaining function and accumulation of regulatory T cells in the colon. Cancer Res 2019; 79: 1178-1190.
[37] Massague J. TGFβeta in cancer. Cell 2008; 134: 215-230.
[38] Yang Y, Weng W, Peng J, Hong L, Yang L, Toiyama Y, Gao R, Liu M, Yin M, Pan C, Li H, Guo B, Zhu Q, Wei Q, Moyer MP, Wang P, Cai S, Goel A, Qin H and Ma Y. Fusobacterium nucleatum increases proliferation of colorectal cancer cells and tumor development in mice by activating toll-like receptor 4 signaling to nuclear factor-kappaB, and up-regulating expression of MicroRNA-21. Gastroenterology 2017; 152: 851-866, e824.
[39] Lamont RJ and Yilmaz O. In or out: the invasiveness of oral bacteria. Periodontol 2000 2002; 30: 61-69.
[40] Hamada S, Amano A, Kimura S, Nakagawa I, Kawabata S and Morisaki I. The importance of fimbriae in the virulence and ecology of some oral bacteria. Oral Microbiol Immunol 1998; 13: 129-138.
[41] Yoshimura F, Murakami Y, Nishikawa K, Hasegawa Y and Kawaminami S. Surface components of porphyromonas gingivalis. J Periodontal Res 2009; 44: 1-12.
[42] Weinberg A, Belton CM, Park Y and Lamont RJ. Role of fimbriae in Porphyromonas gingivalis invasion of gingival epithelial cells. Infect Immun 1997; 65: 313-316.
[43] Xie H, Cai S and Lamont RJ. Environmental regulation of fimbrial gene expression in Porphyromonas gingivalis. Infect Immun 1997; 65: 2265-2271.
[44] Lyons RM, Gentry LE, Purchio AF and Moses HL. Mechanism of activation of latent recombinant transforming growth factor beta 1 by plasmin. J Cell Biol 1990; 110: 1361-1367.
[45] Sato Y and Rifkin DB. Inhibition of endothelial cell movement by pericytes and smooth muscle cells: activation of a latent transforming growth factor-beta 1-like molecule by plasmin during co-culture. J Cell Biol 1989; 109: 309-315.
[46] Yu Q and Stamenkovic I. Cell surface-localized matrix metalloproteinase-9 proteolytically activates TGF-beta and promotes tumor invasion and angiogenesis. Genes Dev 2000; 14: 163-176.
[47] Feldman M, La VD, Lombardo Bedran TB, Palomari Spolidorio DM and Grenier D. Porphyromonas gingivalis-mediated shedding of extracellular matrix metalloproteinase inducer (EMMPRIN) by oral epithelial cells: a potential role in inflammatory periodontal disease. Microbes Infect 2011; 13: 1261-1269.
[48] Fravalo P, Menard C and Bonnaure-Mallet M. Effect of porphyromonas gingivalis on epithelial cell MMP-9 type IV collagenase production. Infect Immun 1996; 64: 4940-4945.
[49] Inaba H, Sugita H, Kuboniwa M, Iwai S, Hamada M, Noda T, Morisaki I, Lamont RJ and Amano A. Porphyromonas gingivalis promotes invasion of oral squamous cell carcinoma through induction of proMMP9 and its activation. Cell Microbiol 2014; 16: 131-145.
[50] Jotwani R, Eswaran SV, Moonga S and Cutler CW. MMP-9/TIMP-1 imbalance induced in human dendritic cells by Porphyromonas gingivalis. FEMS Immunol Med Microbiol 2010; 58: 314-321.
[51] Sun SP, Jin YN, Yang HP, Wei Y and Dong Z. Serum transforming growth factor-beta1 level reflects disease status in patients with esophageal carcinoma after radiotherapy. World J Gastroenterol 2007; 13: 5267-5272.
[52] Miyazono K, Suzuki H and Imamura T. Regulation of TGF-beta signaling and its roles in progression of tumors. Cancer Sci 2003; 94: 230-234.
[53] Nakao A, Imamura T, Souchelnytskyi S, Kawabata M, Ishisaki A, Oeda E, Tamaki K, Hanai J, Heldin CH, Miyazono K and ten Dijke P. TGF-beta receptor-mediated signalling through Smad2, Smad3 and Smad4. EMBO J 1997; 16: 5353-5362.
[54] Girolami I, Veronese N, Smith L, Caruso MG, Reddavide R, Leandro G, Demurtas J and Nottegar A. The activation status of the TGF-beta transducer Smad2 is associated with a reduced survival in gastrointestinal cancers: a systematic review and meta-analysis. Int J Mol Sci 2019; 20: 3831.
[55] Chen Y, Xing P, Chen Y, Zou L, Zhang Y, Li F and Lu X. High p-Smad2 expression in stromal fibroblasts predicts poor survival in patients with clinical stage I to IIIA non-small cell lung cancer. World J Surg Oncol 2014; 12: 328.
[56] Fukuchi M, Nakajima M, Miyazaki T, Masuda N, Osawa H, Manda R, Tsukada K, Kato H and Kuwano H. Lack of activated Smad2 in transforming growth factor-beta signaling is an unfavorable prognostic factor in patients with esophageal squamous cell carcinoma. J Surg Oncol 2006; 94: 51-56.
[57] Mima K, Okabe H, Ishimoto T, Hayashi H, Nakagawa S, Kuroki H, Watanabe M, Beppu T, Tamada M, Nagano O, Saya H and Baba H. CD44s regulates the TGF-beta-mediated mesenchymal phenotype and is associated with

poor prognosis in patients with hepatocellular carcinoma. Cancer Res 2012; 72: 3414-3423.
[58] Wu Y, Li Q, Zhou X, Yu J, Mu Y, Munker S, Xu C, Shen Z, Mullenbach R, Liu Y, Li L, Gretz N, Zieker D, Li J, Matsuzaki K, Li Y, Dooley S and Weng H. Decreased levels of active SMAD2 correlate with poor prognosis in gastric cancer. PLoS One 2012; 7: e35684.
[59] Xie W, Rimm DL, Lin Y, Shih WJ and Reiss M. Loss of Smad signaling in human colorectal cancer is associated with advanced disease and poor prognosis. Cancer J 2003; 9: 302-312.
[60] Park JH, Lee C, Suh JH, Chae JY and Moon KC. Nuclear expression of Smad proteins and its prognostic significance in clear cell renal cell carcinoma. Hum Pathol 2013; 44: 2047-2054.
[61] Yamazaki K, Masugi Y, Effendi K, Tsujikawa H, Hiraoka N, Kitago M, Shinoda M, Itano O, Tanabe M, Kitagawa Y and Sakamoto M. Upregulated SMAD3 promotes epithelial-mesenchymal transition and predicts poor prognosis in pancreatic ductal adenocarcinoma. Lab Invest 2014; 94: 683-691.
[62] Cho SY, Ha SY, Huang SM, Kim JH, Kang MS, Yoo HY, Kim HH, Park CK, Um SH, Kim KH and Kim SH. The prognostic significance of Smad3, Smad4, Smad3 phosphoisoform expression in esophageal squamous cell carcinoma. Med Oncol 2014; 31: 236.
[63] Liu N, Qi D, Jiang J, Zhang J and Yu C. Expression pattern of p-Smad2/Smad4 as a predictor of survival in invasive breast ductal carcinoma. Oncol Lett 2020; 19: 1789-1798.
[64] Ebisawa T, Fukuchi M, Murakami G, Chiba T, Tanaka K, Imamura T and Miyazono K. Smurf1 interacts with transforming growth factor-beta type I receptor through Smad7 and induces receptor degradation. J Biol Chem 2001; 276: 12477-12480.
[65] Han X, Ren J, Lohner H, Yakoumatos L, Liang R and Wang H. SGK1 negatively regulates inflammatory immune responses and protects against alveolar bone loss through modulation of TRAF3 activity. J Biol Chem 2022; 298: 102036.
[66] Maekawa T, Krauss JL, Abe T, Jotwani R, Triantafilou M, Triantafilou K, Hashim A, Hoch S, Curtis MA, Nussbaum G, Lambris JD and Hajishengallis G. Porphyromonas gingivalis manipulates complement and TLR signaling to uncouple bacterial clearance from inflammation and promote dysbiosis. Cell Host Microbe 2014; 15: 768-778.
[67] Fukuchi M, Fukai Y, Masuda N, Miyazaki T, Nakajima M, Sohda M, Manda R, Tsukada K, Kato H and Kuwano H. High-level expression of the Smad ubiquitin ligase Smurf2 correlates with poor prognosis in patients with esophageal squamous cell carcinoma. Cancer Res 2002; 62: 7162-7165.
[68] Hayashi H, Abdollah S, Qiu Y, Cai J, Xu YY, Grinnell BW, Richardson MA, Topper JN, Gimbrone MA Jr, Wrana JL and Falb D. The MAD-related protein Smad7 associates with the TGFβeta receptor and functions as an antagonist of TGFβeta signaling. Cell 1997; 89: 1165-1173.
[69] Nakao A, Afrakhte M, Moren A, Nakayama T, Christian JL, Heuchel R, Itoh S, Kawabata M, Heldin NE, Heldin CH and ten Dijke P. Identification of Smad7, a TGFβeta-inducible antagonist of TGF-beta signalling. Nature 1997; 389: 631-635.
[70] Bitzer M, von Gersdorff G, Liang D, Dominguez-Rosales A, Beg AA, Rojkind M and Bottinger EP. A mechanism of suppression of TGF-beta/SMAD signaling by NF-kappa B/RelA. Genes Dev 2000; 14: 187-197.
[71] Chen W, Jin W, Cook M, Weiner HL and Wahl SM. Oral delivery of group A streptococcal cell walls augments circulating TGF-beta and suppresses streptococcal cell wall arthritis. J Immunol 1998; 161: 6297-6304.
[72] Lee DW, Han SW, Kang JK, Bae JM, Kim HP, Won JK, Jeong SY, Park KJ, Kang GH and Kim TY. Association between fusobacterium nucleatum, pathway mutation, and patient prognosis in colorectal cancer. Ann Surg Oncol 2018; 25: 3389-3395.
[73] Pei Z, Bini EJ, Yang L, Zhou M, Francois F and Blaser MJ. Bacterial biota in the human distal esophagus. Proc Natl Acad Sci U S A 2004; 101: 4250-4255.

Table S2. Clinicopathological characteristics of 190 ESCCs

Name	Gender	Age	Differentiation	Invasion depth	Lymphatic metastasis	status	days	TGFβ1	pSmad2	GARP	P.gingivalis	TNM
XXX	0	1	2	2	0	1	50	0	0	0	0	0
XXX	1	1	2	2	0	1	10	0	1	1	1	0
XXX	1	1	3	2	1	1	32	0	1	1	1	1
XXX	1	0	2	1	0	0	15	0	0	0	0	0
XXX	0	1	1	1	0	0	72	1	0	1	0	0
XXX	1	1	2	2	1	0	72	1	0	1	1	1
XXX	1	1	2	1	0	1	21	0	1	1	0	0
XXX	0	1	1	1	0	0	43	0	0	0	0	0
XXX	1	0	2	2	0	1	7	1	1	1	1	0
XXX	0	0	2	1	0	0	72	1	0	1	0	0
XXX	0	1	1	2	0	1	63	0	0	1	1	0
XXX	1	0	2	2	1	0	66	0	0	0	0	0
XXX	0	0	3	1	1	0	55.9	0	0	0	0	0
XXX	1	1	3	2	1	1	4	0	1	1	1	1
XXX	0	0	2	2	0	0	61.9	0	0	0	0	0
XXX	0	1	3	2	1	1	12.2	0	1	1	1	1
XXX	1	0	2	1	0	1	30	0	0	0	1	0
XXX	0	1	2	1	0	1	42	1	0	0	0	0
XXX	1	0	1	2	1	0	12	0	0	1	0	1
XXX	1	1	2	2	0	0	25	0	1	1	0	0
XXX	0	1	3	2	1	1	11	1	1	0	1	1
XXX	1	0	2	1	1	0	44	0	0	1	0	0
XXX	1	0	2	2	0	0	18	1	0	0	1	0
XXX	1	1	3	2	0	0	20	0	0	0	0	0
XXX	1	1	3	2	0	1	24	1	1	1	1	0
XXX	0	1	2	1	0	1	30	1	1	0	1	0
XXX	1	1	2	1	0	1	32	0	0	0	0	0
XXX	1	1	2	1	0	1	23	1	0	1	0	0
XXX	0	1	2	1	0	1	24	1	0	0	0	0
XXX	1	1	3	2	0	0	72	1	1	0	0	0
XXX	1	1	2	2	0	1	51	0	1	1	0	0
XXX	1	1	1	1	0	1	32	1	1	0	0	0
XXX	1	0	1	2	0	0	24	0	0	0	0	0
XXX	0	1	2	1	0	1	10.1	1	1	0	0	0
XXX	1	1	2	2	1	1	24.9	0	0	1	0	1
XXX	1	1	1	1	0	1	37	1	0	1	0	0
XXX	1	1	1	2	0	0	23	1	1	0	0	0
XXX	0	1	2	1	0	0	61.87	1	1	0	0	0
XXX	1	1	2	1	1	1	17	1	1	1	1	1
XXX	1	1	3	2	1	0	24	0	0	0	1	1
XXX	1	1	2	2	1	0	72	1	0	0	1	1
XXX	1	1	3	2	1	0	21	1	0	1	1	1
XXX	1	0	1	1	1	0	43	1	0	1	0	0
XXX	1	0	2	2	1	1	12	1	0	0	1	1
XXX	1	1	3	2	1	0	20	0	0	0	1	1
XXX	0	0	3	2	0	0	56.85	0	1	1	1	0
XXX	1	0	3	2	1	0	20	1	1	1	1	1
XXX	0	0	2	2	0	0	58.89	1	0	0	1	0
XXX	0	1	3	2	0	0	22	0	1	0	0	0

XXX	1	1	2	2	1	1	29	1	1	1	1	1
XXX	1	1	1	1	1	1	42	0	1	1	1	0
XXX	0	1	2	2	1	0	19	0	1	0	0	1
XXX	1	1	3	2	0	0	18	1	1	0	0	0
XXX	1	0	2	2	0	1	18.3	1	1	0	1	0
XXX	0	1	1	2	0	0	58.89	0	0	0	0	0
XXX	0	1	1	1	0	1	72	0	1	1	0	1
XXX	1	1	3	1	1	1	33	1	0	1	1	0
XXX	0	1	2	1	0	0	43	0	1	0	0	0
XXX	0	0	1	2	0	0	59.9	0	1	0	0	0
XXX	1	1	2	2	0	0	23	0	0	0	0	0
XXX	0	0	1	2	1	1	32	0	1	1	1	1
XXX	0	1	3	1	1	0	23	0	0	1	1	0
XXX	1	0	2	1	1	1	38	0	1	0	1	1
XXX	1	0	2	2	1	1	2	0	1	1	1	1
XXX	1	0	2	2	0	1	18.92	0	1	1	0	0
XXX	0	1	2	1	0	0	20	0	1	0	1	0
XXX	1	1	2	1	0	1	30	0	1	1	0	0
XXX	0	1	1	1	0	1	29	0	0	0	0	0
XXX	1	1	2	1	1	1	9.9	0	1	1	0	1
XXX	1	0	2	1	0	0	43	0	0	0	0	0
XXX	1	0	2	1	1	1	28	0	1	1	1	0
XXX	0	0	1	2	1	1	56	0	1	1	1	1
XXX	0	0	2	1	1	1	14.9	1	1	1	1	0
XXX	0	1	2	1	0	0	56.85	1	0	1	1	0
XXX	1	0	2	1	1	1	29	1	1	1	1	1
XXX	1	1	2	1	1	1	17	0	0	1	1	1
XXX	1	1	2	2	1	1	27	0	0	0	0	1
XXX	1	0	3	1	0	0	56.85	0	1	1	0	0
XXX	0	1	2	1	1	1	13	0	0	0	1	0
XXX	1	1	1	1	1	1	37	1	0	1	1	1
XXX	0	1	2	2	0	1	10	1	0	1	0	0
XXX	1	1	2	2	0	1	10	1	1	1	1	0
XXX	0	1	1	1	0	1	53.93	0	1	0	0	0
XXX	0	1	2	2	0	0	72	0	0	1	0	0
XXX	0	1	2	1	1	1	38	1	0	0	1	1
XXX	1	0	3	1	1	0	22	0	1	0	0	0
XXX	1	0	2	2	0	0	63.8	1	0	1	0	0
XXX	1	1	1	1	0	0	43	1	1	1	1	0
XXX	1	0	1	1	1	0	43	1	0	1	1	1
XXX	1	0	2	2	1	0	72	0	0	1	1	1
XXX	1	1	2	1	0	0	62.9	0	1	0	0	0
XXX	0	1	1	1	0	0	23	0	1	1	0	0
XXX	1	0	1	1	0	0	12	0	1	0	0	0
XXX	1	1	2	1	1	0	42	0	0	0	0	1
XXX	0	1	2	1	0	1	23	0	1	1	0	0
XXX	1	0	2	1	1	1	21.2	0	1	1	0	0
XXX	1	1	2	2	1	0	22	1	0	1	1	1
XXX	1	1	2	1	0	0	42	1	1	0	0	0
XXX	1	1	2	1	0	1	28	1	0	0	0	0
XXX	1	1	3	2	0	0	24	1	1	0	0	0
XXX	1	1	3	1	0	1	6	0	1	1	1	0

XXX	0	0	2	1	0	0	56.85	0	1	1	0	0
XXX	0	1	2	2	0	0	21	0	1	1	0	0
XXX	1	1	3	2	0	0	20	1	1	0	0	0
XXX	1	1	3	2	1	1	26	1	0	0	0	1
XXX	0	1	2	2	1	1	41.9	1	0	1	0	1
XXX	1	1	1	2	1	1	48	0	0	1	1	1
XXX	0	0	1	2	1	1	0.5	0	0	1	1	1
XXX	1	1	2	2	1	1	52	1	1	1	1	1
XXX	1	0	3	1	1	1	31	0	0	0	0	1
XXX	1	0	1	1	0	0	43	0	1	1	0	0
XXX	1	0	1	2	1	1	40	1	1	1	1	1
XXX	1	1	3	2	0	1	29	0	1	1	1	0
XXX	0	1	2	2	0	1	11	1	0	0	0	0
XXX	1	0	2	1	0	0	43	0	1	1	0	0
XXX	1	1	2	1	1	0	43	0	0	0	0	1
XXX	0	1	1	1	0	1	33	0	0	0	1	0
XXX	0	1	2	1	0	1	16.9	1	0	1	0	0
XXX	0	0	2	2	1	1	64	1	1	0	1	1
XXX	1	1	3	1	0	1	3.1	0	1	0	1	0
XXX	0	1	2	2	0	1	5.1	0	0	0	0	0
XXX	1	1	1	1	1	1	23	0	0	0	0	1
XXX	1	1	1	2	0	0	72	0	1	0	0	0
XXX	0	0	2	2	0	0	23	0	1	0	0	0
XXX	1	0	1	2	0	1	13	0	1	1	1	0
XXX	1	1	2	1	1	0	43	0	0	0	0	1
XXX	1	1	3	2	0	0	23	0	1	0	1	0
XXX	1	0	2	1	0	0	59.87	0	1	0	1	0
XXX	1	0	2	1	0	0	41	1	1	1	1	0
XXX	1	0	2	2	1	0	42	1	0	0	1	0
XXX	1	0	1	1	0	0	23	1	0	0	0	0
XXX	0	1	1	2	0	0	72	0	0	0	0	0
XXX	1	1	2	1	0	0	72	0	0	0	0	0
XXX	1	0	2	1	0	0	72	0	0	0	0	0
XXX	0	1	2	1	1	0	72	0	1	1	0	0
XXX	0	0	2	1	0	0	43	1	1	1	0	0
XXX	0	1	1	1	0	0	72	0	1	0	0	0
XXX	1	1	1	2	0	1	38	1	1	1	1	0
XXX	1	1	2	1	1	0	41	0	1	1	1	1
XXX	1	1	2	2	1	1	18	1	1	0	1	1
XXX	1	0	1	2	0	0	63.8	1	0	1	1	0
XXX	1	1	2	1	1	0	42	0	1	1	0	1
XXX	1	1	2	1	1	0	42	0	0	0	0	0
XXX	0	1	2	1	0	0	43	1	1	0	0	0
XXX	1	1	3	2	0	1	11	1	1	1	1	0
XXX	1	0	2	2	1	1	64	0	1	1	1	1
XXX	1	1	2	1	0	0	42	1	1	1	1	0
XXX	0	1	2	1	0	0	42	1	0	0	0	0
XXX	1	0	3	2	0	0	22	0	0	0	0	0
XXX	1	0	3	2	0	0	25	0	0	0	0	0
XXX	1	0	1	1	0	0	42	0	0	0	0	0
XXX	1	1	2	1	0	0	61.9	0	1	0	0	0
XXX	1	0	1	2	0	0	59.9	1	0	1	1	0

XXX	0	1	1	2	0	0	72	0	0	1	0	0
XXX	1	1	2	2	0	1	56.9	0	0	0	0	0
XXX	1	0	3	1	0	0	43	1	1	0	0	0
XXX	0	1	3	1	0	0	19	0	1	1	0	0
XXX	1	1	2	1	1	0	42	0	1	1	0	1
XXX	1	1	2	1	1	1	41	1	1	1	1	0
XXX	1	0	2	2	1	1	47	0	1	1	1	1
XXX	1	1	2	2	0	1	33.9	0	1	1	0	0
XXX	0	1	3	2	1	0	20	0	1	0	1	1
XXX	1	1	1	2	0	1	31.9	1	1	0	0	0
XXX	1	1	3	2	0	0	21	0	0	0	0	0
XXX	1	1	2	2	0	1	38.9	0	1	0	1	0
XXX	1	0	2	1	0	0	58.89	0	0	1	1	0
XXX	0	0	3	1	0	0	23	0	0	0	0	0
XXX	1	1	2	1	1	1	20	0	1	1	0	1
XXX	1	1	2	1	1	0	42	0	0	0	1	1
XXX	1	0	2	2	0	0	58.89	0	0	1	0	1
XXX	1	0	3	2	1	0	24	1	1	1	1	1
XXX	1	1	2	1	0	0	63.8	0	0	0	0	0
XXX	0	1	2	2	0	0	18	1	0	0	0	0
XXX	0	1	2	2	0	1	35	1	0	1	0	0
XXX	1	1	3	2	0	0	72	0	0	1	0	0
XXX	1	1	2	1	0	0	24	0	0	0	0	0
XXX	0	1	1	1	0	1	39.9	1	0	0	0	0
XXX	1	1	1	1	1	1	10	0	0	0	1	0
XXX	1	1	1	2	0	1	64	1	1	1	0	0
XXX	1	1	1	2	0	1	33	0	0	1	0	0
XXX	1	1	1	2	1	1	64	0	0	0	1	1
XXX	1	1	2	1	1	1	19	0	0	0	1	1
XXX	1	1	2	2	0	1	18	0	0	0	0	0
XXX	1	1	2	1	1	0	42	0	1	0	1	0
XXX	1	1	1	2	1	1	15	1	1	0	1	1
XXX	1	1	2	1	0	1	54	0	0	0	0	0
XXX	1	0	2	2	0	1	23.9	0	1	1	1	0
XXX	1	1	1	2	0	1	38	0	1	1	1	0
XXX	1	1	2	2	1	1	10	1	1	1	0	1
XXX	0	0	2	2	0	0	19	1	0	0	0	0

Table S3. Primer sequences used in this study

Primer	Sequence
PAI-1/F	CATAGTCTCAGCCCGCATGG
PAI-1/R	GGGTCAGGGTTCCATCACTT
Smad7/F	CCCCATCACCTTAGCCGACTCTGC
Smad7/R	CCCAGGGGCCAGATAATTCGTTCC
SNAI1/F	CCTGTCTGCGTGGGTTTTTG
SNAI1/R	ACCTGGGGGTGGATTATTGC
Oct4/F	CAAGCTCCTGAAGCAGAAGAGGAT
Oct4/R	CTCACTCGGTTCTCGATACTGGTT
DAPK/F	TGGGAAGCGGAGCTGAAGTG
DAPK/R	CACGGCATTTCTTCACAACCG
BMF/F	CCCTCCTTCCCAATCGAGTC
BMF/R	TCCCCATCCTCTGGTTGGAA
CDKN2B/F	CAACGGAGTCAACCGTTTCG
CDKN2B/R	GGGCAGCATCATGCACCG
p21/F	ACTCTCAGGGTCGAAAACGG
p21/R	ATGTAGAGCGGGCCTTTGAG
BIM/F	GCTACCAGATCCCCACTTTTCA
BIM/R	CTGGGCTCCTGTCTGTGT

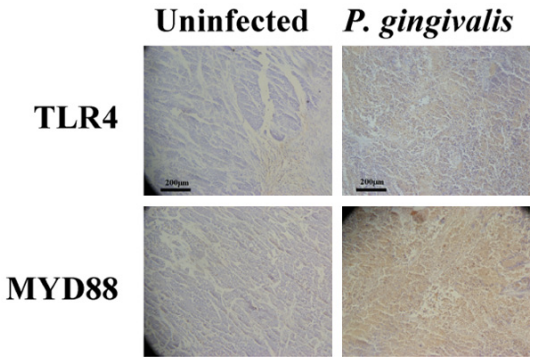

Figure S1. *P. gingivalis*-mediated upregulation of GARP enhances TGFβ activation through TLR4/MYD88 signaling. Representative images of IHC staining of TLR4 and MYD88 in NE6-T-derived xenograft tumors under different treatment conditions. Scale bars, 200 μm.

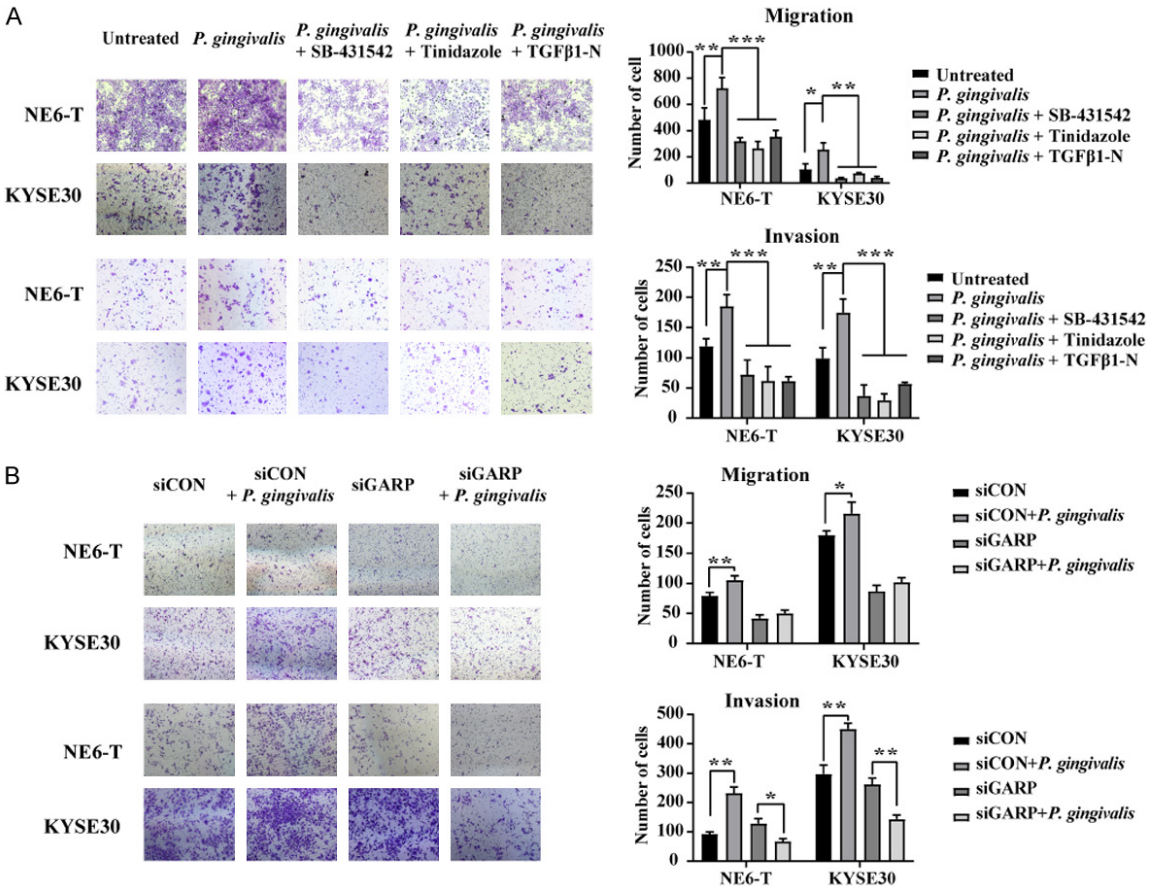

Figure S2. *P. gingivalis* enhances the migration and invasion of NE6-T and KYSE30 cells through GARP upregulation. A, B. Representative images and the quantitation of migration and invasion assay in NE6-T and KYSE30 cells under different treatment conditions. All experiments were independently repeated three times. The quantitation data were presented as means ± SD from three independent experiment with a two-tailed Student's *t*-test for statistical analysis (**P* < 0.05, ***P* < 0.01, and ****P* < 0.001).